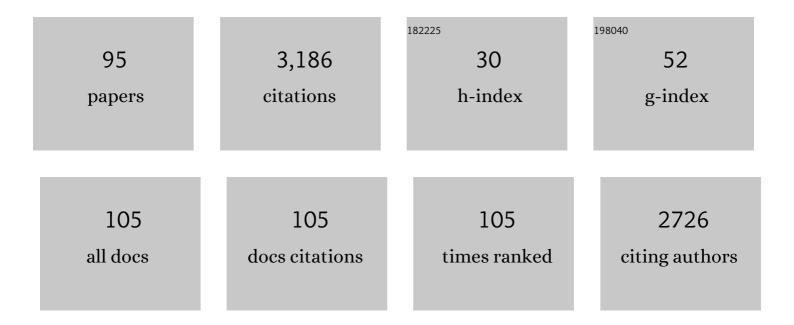
Enrico Dall'Ara

List of Publications by Year in descending order

Source: https://exaly.com/author-pdf/7885245/publications.pdf Version: 2024-02-01



#	Article	IF	CITATIONS
1	MicroFE models of porcine vertebrae with induced bone focal lesions: Validation of predicted displacements with digital volume correlation. Journal of the Mechanical Behavior of Biomedical Materials, 2022, 125, 104872.	1.5	13
2	Geroprotectors and Skeletal Health: Beyond the Headlines. Frontiers in Cell and Developmental Biology, 2022, 10, 682045.	1.8	1
3	Bone biomechanics. , 2022, , 97-120.		1
4	A practical guide for in situ mechanical testing of musculoskeletal tissues using synchrotron tomography. Journal of the Mechanical Behavior of Biomedical Materials, 2022, 133, 105297.	1.5	11
5	Optimization of the failure criterion in micro-Finite Element models of the mouse tibia for the non-invasive prediction of its failure load in preclinical applications. Journal of the Mechanical Behavior of Biomedical Materials, 2021, 113, 104190.	1.5	9
6	Non-invasive prediction of the mouse tibia mechanical properties from microCT images: comparison between different finite element models. Biomechanics and Modeling in Mechanobiology, 2021, 20, 941-955.	1.4	13
7	Damage tolerance and toughness of elderly human femora. Acta Biomaterialia, 2021, 123, 167-177.	4.1	13
8	Subchondral bone microarchitecture and mineral density in human osteoarthritis and osteoporosis: A regional and compartmental analysis. Journal of Orthopaedic Research, 2021, 39, 2568-2580.	1.2	9
9	Patient-Specific Finite Element Models of Posterior Pedicle Screw Fixation: Effect of Screw's Size and Geometry. Frontiers in Bioengineering and Biotechnology, 2021, 9, 643154.	2.0	14
10	The Role of the Loading Condition in Predictions of Bone Adaptation in a Mouse Tibial Loading Model. Frontiers in Bioengineering and Biotechnology, 2021, 9, 676867.	2.0	5
11	A novel approach to evaluate the effects of artificial bone focal lesion on the three-dimensional strain distributionsÂwithin the vertebral body. PLoS ONE, 2021, 16, e0251873.	1.1	10
12	Scientific and regulatory evaluation of mechanistic <i>in silico</i> drug and disease models in drug development: Building model credibility. CPT: Pharmacometrics and Systems Pharmacology, 2021, 10, 804-825.	1.3	51
13	Positive interactions of mechanical loading and PTH treatments on spatio-temporal bone remodelling. Acta Biomaterialia, 2021, 136, 291-305.	4.1	11
14	Type, size, and position of metastatic lesions explain the deformation of the vertebrae under complex loading conditions. Bone, 2021, 151, 116028.	1.4	8
15	High bone mass phenotype in a cohort of patients with Osteogenesis Imperfecta caused due to BMP1 and C-propeptide cleavage variants in COL1A1. Bone Reports, 2021, 15, 101102.	0.2	2
16	Analysis of mechanotransduction dynamics during combined mechanical stimulation and modulation of the extracellular-regulated kinase cascade uncovers hidden information within the signalling noise. Interface Focus, 2021, 11, 20190136.	1.5	6
17	Subchondral Bone Microarchitectural and Mineral Properties and Expression of Key Degradative Proteinases by Chondrocytes in Human Hip Osteoarthritis. Biomedicines, 2021, 9, 1593.	1.4	0
18	A novel algorithm to predict bone changes in the mouse tibia properties under physiological conditions. Biomechanics and Modeling in Mechanobiology, 2020, 19, 985-1001.	1.4	31

#	Article	IF	CITATIONS
19	Heterogeneous Strain Distribution in the Subchondral Bone of Human Osteoarthritic Femoral Heads, Measured with Digital Volume Correlation. Materials, 2020, 13, 4619.	1.3	15
20	Bone remodelling in the mouse tibia is spatio-temporally modulated by oestrogen deficiency and external mechanical loading: A combined in vivo/in silico study. Acta Biomaterialia, 2020, 116, 302-317.	4.1	28
21	Full-field comparisons between strains predicted by QCT-derived finite element models of the scapula and experimental strains measured by digital volume correlation. Journal of Biomechanics, 2020, 113, 110101.	0.9	7
22	Development of Subject Specific Finite Element Models of the Mouse Knee Joint for Preclinical Applications. Frontiers in Bioengineering and Biotechnology, 2020, 8, 558815.	2.0	6
23	Regional and compartmentalized variation of subchondral bone mineralization and microarchitecture in hip osteoarthritis. Osteoarthritis and Cartilage, 2020, 28, S174.	0.6	0
24	PTH(1–34) treatment and/or mechanical loading have different osteogenic effects on the trabecular and cortical bone in the ovariectomized C57BL/6 mouse. Scientific Reports, 2020, 10, 8889.	1.6	17
25	The Application of Digital Volume Correlation (DVC) to Evaluate Strain Predictions Generated by Finite Element Models of the Osteoarthritic Humeral Head. Annals of Biomedical Engineering, 2020, 48, 2859-2869.	1.3	8
26	Regional Nanoindentation Properties in Different Locations on the Mouse Tibia From C57BL/6 and Balb/C Female Mice. Frontiers in Bioengineering and Biotechnology, 2020, 8, 478.	2.0	10
27	Effect of size and location of simulated lytic lesions on the structural properties of human vertebral bodies, a micro-finite element study. Bone Reports, 2020, 12, 100257.	0.2	14
28	Revealing hidden information in osteoblast's mechanotransduction through analysis of time patterns of critical events. BMC Bioinformatics, 2020, 21, 114.	1.2	4
29	ChronoMID—Cross-modal neural networks for 3-D temporal medical imaging data. PLoS ONE, 2020, 15, e0228962.	1.1	0
30	A new approach to comprehensively evaluate the morphological properties of the human femoral head: example of application to osteoarthritic joint. Scientific Reports, 2020, 10, 5538.	1.6	11
31	AB0076â€SPATIAL VARIATIONS OF BONE MICROARCHITECTURE AND MINERALIZATION IN HIP OSTEOARTHRITI AND OSTEOPOROSIS. Annals of the Rheumatic Diseases, 2020, 79, 1338.2-1338.	S _{0.5}	0
32	A new method to monitor bone geometry changes at different spatial scales in the longitudinal in vivo μCT studies of mice bones. PLoS ONE, 2019, 14, e0219404.	1.1	3
33	Material Mapping of QCT-Derived Scapular Models: A Comparison with Micro-CT Loaded Specimens Using Digital Volume Correlation. Annals of Biomedical Engineering, 2019, 47, 2188-2198.	1.3	13
34	The longitudinal effects of ovariectomy on the morphometric, densitometric and mechanical properties in the murine tibia: A comparison between two mouse strains. Bone, 2019, 127, 260-270.	1.4	35
35	Biomechanical assessment of vertebrae with lytic metastases with subject-specific finite element models. Journal of the Mechanical Behavior of Biomedical Materials, 2019, 98, 268-290.	1.5	29
36	Prenatal growth map of the mouse knee joint by means of deformable registration technique. PLoS ONE, 2019, 14, e0197947.	1.1	1

#	Article	IF	CITATIONS
37	Uncertainties of synchrotron microCT-based digital volume correlation bone strain measurements under simulated deformation. Journal of Biomechanics, 2019, 86, 232-237.	0.9	17
38	Performance of QCT-Derived scapula finite element models in predicting local displacements using digital volume correlation. Journal of the Mechanical Behavior of Biomedical Materials, 2019, 97, 339-345.	1.5	22
39	Analysis of Bone Architecture in Rodents Using Micro-Computed Tomography. Methods in Molecular Biology, 2019, 1914, 507-531.	0.4	11
40	Full-Field Strain Analysis of Bone–Biomaterial Systems Produced by the Implantation of Osteoregenerative Biomaterials in an Ovine Model. ACS Biomaterials Science and Engineering, 2019, 5, 2543-2554.	2.6	23
41	Effect of repeated in vivo microCT imaging on the properties of the mouse tibia. PLoS ONE, 2019, 14, e0225127.	1.1	18
42	From bed to bench: How in silico medicine can help ageing research. Mechanisms of Ageing and Development, 2019, 177, 103-108.	2.2	25
43	Comparison of femoral strength and fracture risk index derived from DXA-based finite element analysis for stratifying hip fracture risk: A cross-sectional study. Bone, 2018, 110, 386-391.	1.4	11
44	Validation of calcaneus trabecular microstructure measurements by HR-pQCT. Bone, 2018, 106, 69-77.	1.4	18
45	Preservation of Bone Tissue Integrity with Temperature Control for In Situ SR-MicroCT Experiments. Materials, 2018, 11, 2155.	1.3	16
46	Variability in strain distribution in the mice tibia loading model: A preliminary study using digital volume correlation. Medical Engineering and Physics, 2018, 62, 7-16.	0.8	19
47	Validation of finite element models of the mouse tibia using digital volume correlation. Journal of the Mechanical Behavior of Biomedical Materials, 2018, 86, 172-184.	1.5	52
48	Mapping anisotropy improves QCT-based finite element estimation of hip strength in pooled stance and side-fall load configurations. Medical Engineering and Physics, 2018, 59, 36-42.	0.8	13
49	Comparison of HR-pQCT- and microCT-based finite element models for the estimation of the mechanical properties of the calcaneus trabecular bone. Biomechanics and Modeling in Mechanobiology, 2018, 17, 1715-1730.	1.4	12
50	Effect of SR-microCT radiation on the mechanical integrity of trabecular bone using in situ mechanical testing and digital volume correlation. Journal of the Mechanical Behavior of Biomedical Materials, 2018, 88, 109-119.	1.5	55
51	Strain uncertainties from two digital volume correlation approaches in prophylactically augmented vertebrae: Local analysis on bone and cement-bone microstructures. Journal of the Mechanical Behavior of Biomedical Materials, 2017, 67, 117-126.	1.5	47
52	Longitudinal effects of Parathyroid Hormone treatment on morphological, densitometric and mechanical properties of mouse tibia. Journal of the Mechanical Behavior of Biomedical Materials, 2017, 75, 244-251.	1.5	33
53	Local displacement and strain uncertainties in different bone types by digital volume correlation of synchrotron microtomograms. Journal of Biomechanics, 2017, 58, 27-36.	0.9	43
54	Micro-CT based finite element models of cancellous bone predict accurately displacement once the boundary condition is well replicated: A validation study. Journal of the Mechanical Behavior of Biomedical Materials, 2017, 65, 644-651.	1.5	81

#	Article	IF	CITATIONS
55	Effect of integration time on the morphometric, densitometric and mechanical properties of the mouse tibia. Journal of Biomechanics, 2017, 65, 203-211.	0.9	26
56	Precision of Digital Volume Correlation Approaches for Strain Analysis in Bone Imaged with Micro-Computed Tomography at Different Dimensional Levels. Frontiers in Materials, 2017, 4, .	1.2	58
57	Micro Finite Element models of the vertebral body: Validation of local displacement predictions. PLoS ONE, 2017, 12, e0180151.	1.1	55
58	The Initial Slope of the Variogram, Foundation of the Trabecular Bone Score, Is Not or Is Poorly Associated With Vertebral Strength. Journal of Bone and Mineral Research, 2016, 31, 341-346.	3.1	26
59	Rotational stability in screw-fixed scaphoid fractures compared to plate-fixed scaphoid fractures. Archives of Orthopaedic and Trauma Surgery, 2016, 136, 1623-1628.	1.3	57
60	Longitudinal imaging of the ageing mouse. Mechanisms of Ageing and Development, 2016, 160, 93-116.	2.2	47
61	Digital volume correlation can be used to estimate local strains in natural and augmented vertebrae: An organ-level study. Journal of Biomechanics, 2016, 49, 3882-3890.	0.9	50
62	Development of a protocol to quantify local bone adaptation over space and time: Quantification of reproducibility. Journal of Biomechanics, 2016, 49, 2095-2099.	0.9	33
63	Experimental validation of DXA-based finite element models for prediction of femoral strength. Journal of the Mechanical Behavior of Biomedical Materials, 2016, 63, 17-25.	1.5	61
64	Evaluation of in-vivo measurement errors associated with micro-computed tomography scans by means of the bone surface distance approach. Medical Engineering and Physics, 2015, 37, 1091-1097.	0.8	20
65	Estimation of local anisotropy of plexiform bone: Comparison between depth sensing micro-indentation and Reference Point Indentation. Journal of Biomechanics, 2015, 48, 4073-4080.	0.9	8
66	Three-Dimensional Local Measurements of Bone Strain and Displacement: Comparison of Three Digital Volume Correlation Approaches. Journal of Biomechanical Engineering, 2015, 137, .	0.6	68
67	Calcium phosphate cement augmentation after volar locking plating of distal radius fracture significantly increases stability. European Journal of Orthopaedic Surgery and Traumatology, 2014, 24, 869-875.	0.6	12
68	Assessment of Transverse Isotropy in Clinical-Level CT Images of Trabecular Bone Using the Gradient Structure Tensor. Annals of Biomedical Engineering, 2014, 42, 950-959.	1.3	29
69	About the inevitable compromise between spatial resolution and accuracy of strain measurement for bone tissue: A 3D zero-strain study. Journal of Biomechanics, 2014, 47, 2956-2963.	0.9	83
70	Clinical versus pre-clinical FE models for vertebral body strength predictions. Journal of the Mechanical Behavior of Biomedical Materials, 2014, 33, 76-83.	1.5	35
71	Orthotropic HR-pQCT-based FE models improve strength predictions for stance but not for side-way fall loading compared to isotropic QCT-based FE models of human femurs. Journal of the Mechanical Behavior of Biomedical Materials, 2014, 32, 287-299.	1.5	44
72	Tissue properties of the human vertebral body sub-structures evaluated by means of microindentation. Journal of the Mechanical Behavior of Biomedical Materials, 2013, 25, 23-32.	1.5	27

#	Article	IF	CITATIONS
73	DXA predictions of human femoral mechanical properties depend on the load configuration. Medical Engineering and Physics, 2013, 35, 1564-1572.	0.8	31
74	A nonlinear QCT-based finite element model validation study for the human femur tested in two configurations in vitro. Bone, 2013, 52, 27-38.	1.4	145
75	Finite element analysis for prediction of bone strength. BoneKEy Reports, 2013, 2, 386.	2.7	130
76	HR-pQCT-based homogenised finite element models provide quantitative predictions of experimental vertebral body stiffness and strength with the same accuracy as μFE models. Computer Methods in Biomechanics and Biomedical Engineering, 2012, 15, 711-720.	0.9	43
77	Removal of the cortical endplates has little effect on ultimate load and damage distribution in QCT-based voxel models of human lumbar vertebrae under axial compression. Journal of Biomechanics, 2012, 45, 1733-1738.	0.9	16
78	Microindentation can discriminate between damaged and intact human bone tissue. Bone, 2012, 50, 925-929.	1.4	39
79	Assessment of a novel biomechanical fracture model for distal radius fractures. BMC Musculoskeletal Disorders, 2012, 13, 252.	0.8	12
80	QCT-based finite element models predict human vertebral strength in vitro significantly better than simulated DEXA. Osteoporosis International, 2012, 23, 563-572.	1.3	142
81	Lathyrism-induced alterations in collagen cross-links influence the mechanical properties of bone material without affecting the mineral. Bone, 2011, 49, 1232-1241.	1.4	112
82	Multidirectional volar fixed-angle plating using cancellous locking screws for distal radius fractures – Evaluation of three screw configurations in an extra-articular fracture model. Wiener Klinische Wochenschrift, 2011, 123, 4-10.	1.0	10
83	Validation of an HR-pQCT-based homogenized finite element approach using mechanical testing of ultra-distal radius sections. Biomechanics and Modeling in Mechanobiology, 2011, 10, 431-444.	1.4	51
84	Reduced tissue hardness of trabecular bone is associated with severe osteoarthritis. Journal of Biomechanics, 2011, 44, 1593-1598.	0.9	33
85	Bone and Cellular Immune System of Multiparous Sows are Insensitive to Ovariectomy and Nutritive Calcium Shortage. Hormone and Metabolic Research, 2011, 43, 404-409.	0.7	13
86	A calibration methodology of QCT BMD for human vertebral body with registered micro-CT images. Medical Physics, 2011, 38, 2602-2608.	1.6	24
87	OPG-Fc Treatment in Growing Pigs Leads to Rapid Reductions in Bone Resorption Markers, Serum Calcium, and Bone Formation Markers. Hormone and Metabolic Research, 2011, 43, 944-949.	0.7	14
88	Volar Fixed-Angle Plating of Extra-Articular Distal Radius Fractures—A Biomechanical Analysis Comparing Threaded Screws and Smooth Pegs. Journal of Trauma, 2010, 69, E46-E55.	2.3	16
89	A nonlinear finite element model validation study based on a novel experimental technique for inducing anterior wedge-shape fractures in human vertebral bodies in vitro. Journal of Biomechanics, 2010, 43, 2374-2380.	0.9	88
90	An accurate estimation of bone density improves the accuracy of subject-specific finite element models. Journal of Biomechanics, 2008, 41, 2483-2491.	0.9	333

#	Article	IF	CITATIONS
91	The effects of embalming using a 4% formalin solution on the compressive mechanical properties of human cortical bone. Clinical Biomechanics, 2008, 23, 1294-1298.	0.5	122
92	The effect of tissue condition and applied load on Vickers hardness of human trabecular bone. Journal of Biomechanics, 2007, 40, 3267-3270.	0.9	41
93	Mechanical testing of cancellous bone from the femoral head: Experimental errors due to off-axis measurements. Journal of Biomechanics, 2007, 40, 2426-2433.	0.9	100
94	Damage Tolerance and Toughness of Elderly Human Femora. SSRN Electronic Journal, 0, , .	0.4	0
95	Reproducibility of Densitometric and Biomechanical Assessment of the Mouse Tibia From In Vivo Micro-CT Images. Frontiers in Endocrinology, 0, 13, .	1.5	1